

Synthesis of 2-Azulenyl-1,1,4,4-tetracyano-3-ferrocenyl-1,3-butadienes by the [2+2] Cycloaddition of (Ferrocenylethynyl)azulenes with Tetracyanoethylene

Taku Shoji,^{*,[a]} Shunji Ito,^[b] Tetsuo Okujima,^[c] and Noboru Morita^[a]

Abstract: 1-, 2-, and 6-(ferrocenylethynyl)azulene derivatives **10–16** have been prepared by palladium-catalyzed alkylation of ethynylferrocene with the corresponding haloazulenes under Sonogashira–Hagihara conditions. Compounds **10–16** reacted with tetracyanoethylene (TCNE) in a [2+2]

cycloaddition–cycloreversion reaction to afford the corresponding 2-azulenyl-1,1,4,4-tetracyano-3-ferrocenyl-1,3-butadiene chromophores **17–23** in excellent yields. The redox behavior of the novel azulene chromophores **17–23** was examined by cyclic voltammetry (CV) and differential pulse voltammetry (DPV), which

revealed their multistep electrochemical reduction properties. Moreover, a significant color change was observed by visible spectroscopy under electrochemical reduction conditions.

Keywords: Azulene • Ferrocene • Cycloaddition • Donor–acceptor system • Electrochemistry

Introduction

Recently, much attention has been focused on donor–acceptor molecules with a multistage redox property because of their special functions such as conductivity and organic ferromagnetism.^[1]

Ferrocene has attracted interest due to its characteristic redox properties, with a low oxidation potential allowing it to produce a stabilized cationic form, ferrocenium ion.^[2] Thus, a large number of donor–acceptor systems possessing a ferrocenyl group have been synthesized and their properties have been extensively studied. In 2002, Mochida et al. reported that the reaction of ethynylferrocene

derivatives with tetracyanoethylene (TCNE) to afford formal [2+2] cycloaddition products, namely the cyclobutene derivatives, which undergo a ring-opening reaction to give the corresponding ferrocene-substituted 1,1,4,4-tetracyano-1,3-butadienes (TCBDs) that show amphoteric redox behavior on cyclic voltammetry (CV).^[3] Diederich et al. also reported that a variety of ferrocene-substituted alkynes and butadiynes react with TCNE and 7,7,8,8-tetracyanoquinodimethane (TCNQ) to give the corresponding TCBDs and dicyanoquinodimethanes (DCNQs) with a ferrocenyl group, respectively, in excellent yields.^[4] More recently, Michinobu reported the reaction of ferrocene-containing poly(aryleneethynylene)s with TCNE to give ferrocene-substituted polyTCBDs, which could be applied to organic optoelectronic devices, such as nonlinear optics and photovoltaics.^[5]

Azulene has attracted the interest of many research groups due to its unusual properties as well as its beautiful blue color.^[6] For the creation of multistage redox system, we have prepared several di(1-azulenyl)ferrocenylmethyl cations, which exhibit amphoteric redox behavior on CV (e.g., facile one-stage oxidation and reduction properties).^[7] We have also examined [2+2] cycloaddition–cycloreversion reaction of mono-, bis-, and tris(1-azulenylethynyl)benzene and the thiophene derivatives with TCNE and TCNQ to give the corresponding TCBDs and DCNQs with intramolecular charge-transfer (ICT) characters in excellent yields. In this study, we have revealed their multistep reduction behavior by CV and differential pulse voltammetry (DPV). Moreover, significant color changes are also observed by the electrochemical reduction of the new chromophores.^[8] However, TCBD derivatives including both azulene and ferrocene substituents are not explored so far. The azulene system has a tendency to stabilize cations, as well as anions, depending on the position substituted through the contributions of its formal tropylium and cyclopentadienide substructures. Indeed, our previous study revealed that the π -electron systems with the 2- or 6-azulenyl

[a] Dr. T. Shoji
Department of Chemistry, Faculty of Science, Shinshu University
Matsumoto 390-8621, Japan
Fax: (+) 81-263-37-2476
E-mail: tshoji@shinshu-u.ac.jp

[b] Prof. Dr. S. Ito
Graduate School of Science and Technology, Hirosaki University
Hirosaki 036-8561, Japan

[c] Dr. T. Okujima
Department of Chemistry and Biology, Graduate School of Science and Engineering, Ehime University
Matsuyama 790-8577, Japan

[d] Prof. Dr. N. Morita
Department of Chemistry, Graduate School of Science, Tohoku University
Sendai 980-8578, Japan

((If supporting information is submitted, please include the following line:))

Supporting information for this article is available on the WWW under <http://www.chemeurj.org/> or from the author.

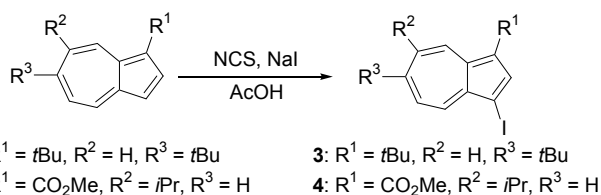
groups also possess these tendencies.^[9] Thus, TCBD derivatives with both azulenyl and ferrocenyl groups should stabilize their amphoteric redox cycles and consequently should improve their electrochromic property, rather than TCBD derivatives substituted by 1-azulenyl group alone.

Herein, we describe the palladium-catalyzed synthesis of 1-, 2-, and 6-(ferrocenylethynyl)azulenes, as well as transformation of the ethynylazulenes to novel TCBD derivatives by [2+2] cycloaddition–cycloreversion reaction with TCNE. The electronic properties of the new donor–acceptor chromophores obtained by these reactions were characterized by CV, DPV, and absorption spectroscopy. The data confirm the powerful ICT character of the novel TCBD chromophores bearing both azulene and ferrocene substituents with respect to their optoelectronic properties.

Results and Discussion

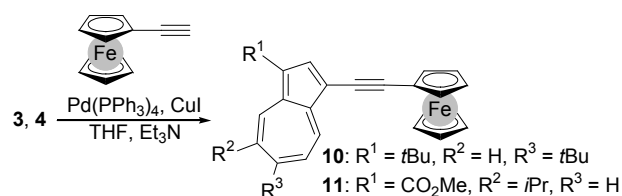
Synthesis of (ferrocenylethynyl)azulenes

Iodine is a very important substituent in the transition-metal-catalyzed cross-coupling reaction of aromatic compounds. 1-Iodoazulene derivatives are usually prepared by the reaction of *N*-iodosuccinimide (NIS) with the corresponding azulene derivatives, although NIS is a rather expensive reagent. Thus, we examined a new iodination procedure using *N*-chlorosuccinimide (NCS) and NaI, to prepare the 1-iodoazulene derivatives **3** and **4** for the palladium-catalyzed cross-coupling reaction.^[10] The reaction of 1,6-di-*tert*-butylazulene (**1**)^[11] and methyl 7-isopropylazulene-1-carboxylate (**2**)^[12] with NCS/NaI in acetic acid at room temperature afforded the corresponding 1-iodoazulene derivatives **3** and **4** in 94% and 96% yields, respectively (Scheme 1). The yields of the products were slightly improved by this procedure compared with those from the reaction with NIS.^[8,14] Thus, the new procedure has advantages for the preparation of 1-iodoazulene derivatives, with respect to the product yields and cost-effectiveness.



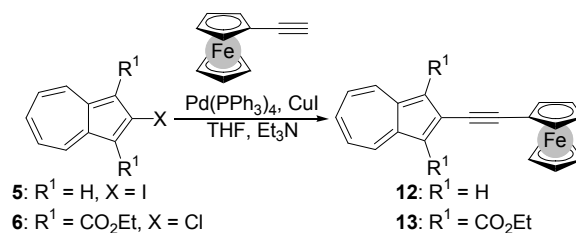
Scheme 1.

Preparation of (ferrocenylethynyl)azulenes **10–16** was accomplished by palladium-catalyzed alkylation of ethynylferrocene with the corresponding haloazulenes **3–9** under the Sonogashira–Hagihara conditions.^[13] The cross-coupling reaction of ethynylferrocene with 1,6-di-*tert*-butyl-3-iodoazulene (**3**)^[14] in the presence of Pd(PPh₃)₄ as a catalyst in THF/Et₃N at 50 °C gave 1,6-di-*tert*-butyl-3-(ferrocenylethynyl)azulene (**10**) in 92% yield. The cross-coupling reaction of **4**^[18] with ethynylferrocene using Pd(PPh₃)₄ as a catalyst and subsequent chromatographic purification on silica gel afforded the desired methyl 3-(ferrocenylethynyl)-7-isopropylazulene-1-carboxylate (**11**) in 96% yield (Scheme 2).

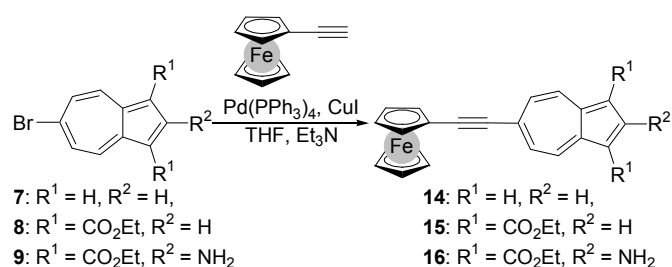


Scheme 2.

Likewise, the reaction of 2-iodoazulene (**5**)^[15] with ethynylferrocene afforded 2-(ferrocenylethynyl)azulene (**12**) in 96% yield. Reaction of diethyl 2-chloroazulene-1,3-dicarboxylate (**6**) with ethynylferrocene afforded **13** in 92% yield, although aryl chloride is usually less reactive toward the palladium-catalyzed cross-coupling reaction compared with that of aryl iodide and bromide (Scheme 3).^[16] High yield of the product **13** should be responsible to the electron-withdrawing nature of the 1,3-diethoxycarbonyl groups on the azulene ring, which should increase the reactivity toward the oxidative addition of the palladium catalyst. The cross-coupling reaction of 6-bromoazulene (**6**)^[17] with ethynylferrocene in the presence of the palladium-catalyst afforded 6-(ferrocenylethynyl)azulene (**14**) in 99% yield. As similar with the reactions described above, Sonogashira–Hagihara reaction of ethynylferrocene with 6-bromoazulene derivatives **8**^[4] and **9**^[18] gave the corresponding cross-coupled products **15** and **16** in 97% and 95% yields, respectively (Scheme 4).



Scheme 3.

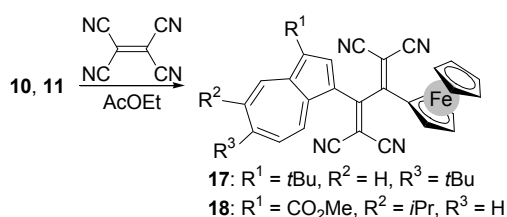


Scheme 4.

These (ferrocenylethynyl)azulenes **10–16** possess fair solubility toward general organic solvents, such as chloroform, dichloromethane, and so on. Moreover, they are stable and showing no decomposition even after several weeks at room temperature. Thus, the (ferrocenylethynyl)azulenes **10–16** were utilized in further transformation on the synthesis of the novel TCBD derivatives bearing both azulene and ferrocene substituents owing to their considerable stability and solubility.

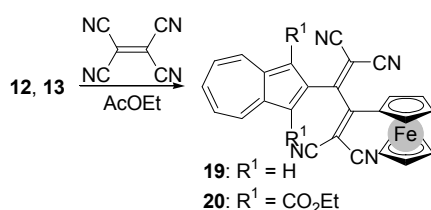
[2+2] Cycloaddition–cycloreversion reaction of (ferrocenylethynyl)azulenes with tetracyanoethylene

For the synthesis of novel ferrocene-substituted TCBD derivatives, [2+2] cycloaddition–cycloreversion sequence of **10–16** with TCNE was examined according to the procedure described in the literatures.^[3,4,8] The reaction of **10**, that has electron-donating *tert*-butyl groups at the 1,6-positions on the azulene ring, with TCNE in ethyl acetate at room temperature yielded **17** in 92% yield. Acetylene derivative **11**, which possesses an electron-withdrawing methoxycarbonyl group at the 1-position on the azulene ring, also reacted readily with TCNE, as similar with the reaction of **10**, to afford the corresponding TCBD derivative **18** in 97% yield (Scheme 5).

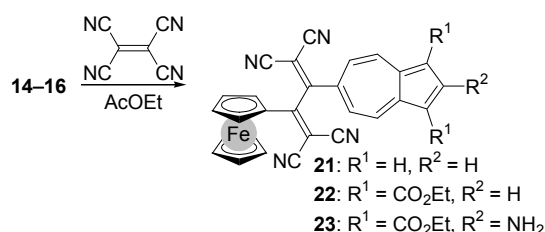


Scheme 5.

Likewise, the [2+2] cycloaddition–cycloreversion sequence of **12** with TCNE in ethyl acetate at room temperature afforded **19** in 93% yield. Although the 2-(ferrocenylethynyl)azulene **13** with 1,3-diethoxycarbonyl substituents did not react with TCNE at room temperature, desired cycloadduct **20** was obtained in 89% yield under the refluxing conditions in ethyl acetate (Scheme 6). The low reactivity of the (ferrocenylethynyl)azulene toward TCNE might be attributable to both electron-withdrawing property and steric hindrance of the two ethoxycarbonyl groups at the 1,3-positions. 6-(Ferrocenylethynyl)azulenes **14**, **15**, and **16** also reacted with TCNE in refluxing ethyl acetate to afford the corresponding [2+2] cycloaddition products **21**, **22**, and **23** in 91%, 88%, and 93% yields, respectively (Scheme 7). The reaction of 2-phenylethynyl and 6-phenylethynylazulenes with TCNE was also investigated under the similar reaction conditions, but the reaction did not afford the desired TCBD derivatives. These results indicate reactivity of the acetylene moiety is not increased by the 2-azulenyl- and 6-azulenyl-substituents, because these groups do not behave as good electron-donating groups. Thus, the other highly electron-donating substituent is necessary on acetylene moiety to proceed with the [2+2] cycloaddition reaction of 2-ethynyl- and 6-ethynylazulene derivatives. The new TCBD chromophores bearing azulene and ferrocene substituents **17–23** are stable, deep-colored crystals, and are storable in crystalline state at ambient temperature under aerobic conditions.



Scheme 6.



Scheme 7.

Spectroscopic Property: These new compounds **10–23** were fully characterized by the spectral data as summarized in the Experimental Section. The NMR assignment of the reported compounds was confirmed by the HMQC, HMBC, and NOE experiments, and so on. High resolution mass spectra of **10–23** ionized by ESI or FAB showed the correct molecular ion peaks. The characteristic stretching-vibration band of the C≡N moiety of TCBDs **17–23** was observed at 2208 to 2220 cm⁻¹ on their IR spectra. These results are consistent with the structure of these products.

The UV–visible spectra of **10–16** showed characteristic weak absorptions arising from the azulene system in the visible region. UV–visible spectra of **17** and **21–23** are shown in Figures 1 and 2, respectively. Absorption maxima and coefficients (log ε) of **17–23** are summarized in Table 1. Compound **17** exhibited a broad and strong CT absorption centered at λ_{max} = 492 nm, which reached up to 900 nm (Figure 1). Previously, Mochida et al. reported that 2,5-dicyano-3-ferrocenylhexa-2,4-dienedinitrile (Figure 3) exhibits broad absorption at λ_{max} = 632 nm in dichloromethane. They concluded the absorption band as ICT arising from the π–π* transition between ferrocene and TCBD moieties.^[3] Therefore, the broad absorption of **17** should be ascribed to overlapping the two-types of ICT absorptions from ferrocene and azulene moieties to the TCBD unit. The solvent dependence of the absorption spectra of **17** was also shown in Figure 1. The absorption band of **17** exhibits slight blue shift by the addition of hexane to dichloromethane, which suggests the ICT nature of this band.^[19] Likewise, TCBD **18** with a 1-azulenyl substituent also displayed a broad and a strong CT absorption bands at λ_{max} = 459 nm and 644 (sh) nm, respectively. When the solvent was changed to 10% CH₂Cl₂/hexane from CH₂Cl₂, absorption band at λ_{max} = 459 nm showed a slight hypsochromic shift by 8 nm (λ_{max} = 451 nm). However, the longest wavelength absorption maximum at λ_{max} = 644 (sh) nm in CH₂Cl₂ exhibited rather large blue-shift to λ_{max} = 597 (sh) nm in less-polar 10% CH₂Cl₂/hexane. Thus, the ICT from ferrocene to the TCBD moiety is assumed to be more sensitive toward the polarity of solvent than that from 1-azulenyl group to the TCBD unit.

TCBD **19** with a 2-azulenyl substituent showed a strong and a broad CT absorption bands at λ_{max} = 402 nm and 616 nm, respectively, arising from the ICT from both azulene and ferrocene to TCBD unit. However, compound **20** did not afford similar two absorption bands on the UV–visible spectrum, but exhibit a broad absorption band in the visible region. These results indicate the less effective conjugation between azulene and TCBD moieties owing to the steric effect of 1,3-diethoxycarbonyl groups.

The UV–visible spectra of the TCBD derivatives **21**, **22**, and **23** with a 6-azulenyl substituent exhibited a weak-broad absorption

band at $\lambda_{\text{max}} = 638 \text{ nm}$, 621 nm , and 640 nm , respectively, which reflect the CT absorption band between ferrocene and TCBD moieties (Figure 2). A strong absorption band in the visible region ($\lambda_{\text{max}} = 499 \text{ nm}$) was also observed in **23**, although **21** and **22** did not show such an absorption band. Contribution of the resonance structure in **23** with azulene quinoid form^[20] by the effect of 2-amino moiety as illustrated in Scheme 8 should be responsible to the absorption band.

Table 1. Absorption maxima [nm] and their coefficients ($\log \epsilon$) of TCBDs **17–24** in CH_2Cl_2 and in 10% $\text{CH}_2\text{Cl}_2/\text{hexane}$.

Sample	λ_{max} [nm], ($\log \epsilon$) ^[a] in CH_2Cl_2	λ_{max} [nm], ($\log \epsilon$) ^[a] in hexane ^[b]
17	492 (4.16), 590 sh (3.62)	484 (4.20), 590 sh (3.62)
18	459 (4.10), 644 sh (3.31)	451 (4.21), 547 sh (3.54), 597 sh (3.52)
19	402 (4.41), 427 sh (4.17), 616 (3.48)	399 (4.38), 420 sh (4.10), 590 (3.43)
20	556 (3.24), 753 (3.07)	553 (3.28), 724 (3.14)
21	394 sh (4.06), 638 (3.43)	385 sh (4.07), 620 (3.42)
22	380 sh (4.28), 621 (3.47)	378 sh (4.28), 603 (3.52)
23	408 sh (4.04), 499 (4.28), 640 sh (3.38)	406 sh (4.02), 492 (4.32), 616 sh (3.37)
24 ^[3]	350 (3.98), 632 (3.32)	344 (3.98), 611 (3.30)

[a] sh = shoulder peak. [b] Dichloromethane (10%) was contained to maintain the solubility of these compounds.

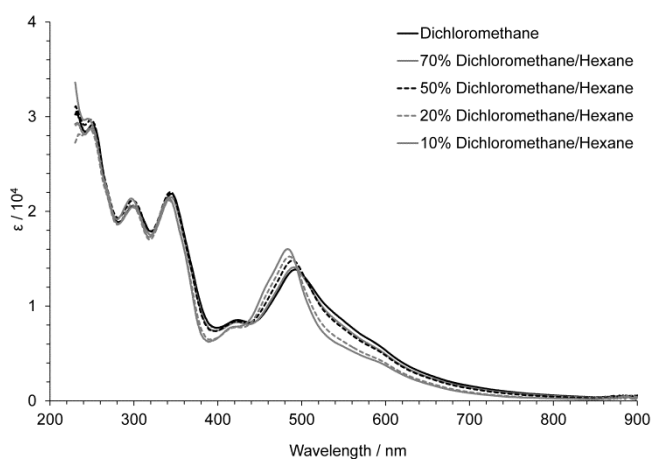


Figure 1. Solvent dependence of UV/Vis spectrum of **17** in CH_2Cl_2 and in $\text{CH}_2\text{Cl}_2/\text{hexane}$.

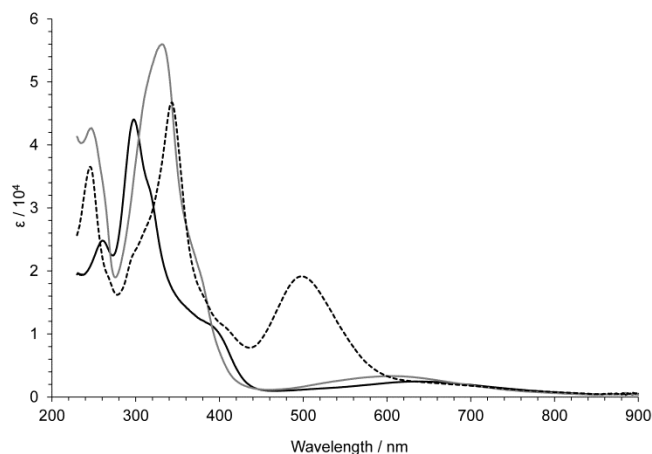
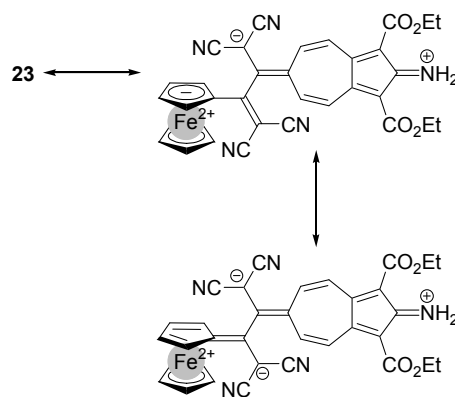


Figure 2. UV/Vis spectra of **21** (black line), **22** (gray line), and **23** (broken line) in CH_2Cl_2 .



Figure 3. 2,5-Dicyano-3-ferrocenylhexa-2,4-dienedinitrile (**24**).



Scheme 8.

Electrochemistry: To clarify the effect of substituents and substitution position on the azulene ring in the TCBD derivatives including a ferrocenyl group toward electrochemical properties, the redox behavior of TCBDs **17–24** was examined by CV and DPV. Measurements were carried out with a standard three-electrode configuration. We utilize benzonitrile as a solvent for the electrochemical studies because of the solubility of the samples and also good conductivity under the measurement conditions which has an advantage in the electrochromic study. Tetraethylammonium perchlorate (0.1 M) in benzonitrile was used as a supporting electrolyte with platinum wire auxiliary and disk working electrodes. All measurements were carried out under an argon atmosphere, and the potentials were related to a standard Ag/AgNO_3 reference electrode. Half-wave potential of ferrocene–ferrocenium ion couple (Fc/Fc^+) under the conditions using this reference electrode is observed at +0.15 V on CV. The accuracy of the reference electrode was confirmed by the CV measurement of the couple in each sample

as an internal ferrocene standard. The redox potentials (in volts vs. Ag/AgNO₃) of **17–24** measured under the scan rate of 100 mVs⁻¹ are summarized in Table 2. In the case of reversible waves, redox potentials measured by CV are presented. The peak potentials measured by DPV are shown in parentheses. The half-wave potentials of **17–24** for ferrocene standard may calculate by subtraction from the presented values by 0.15 V regarded as the half-wave potential of ferrocene–ferrocenium ion couple. All TCBD chromophores **17–24** showed reversible one-stage oxidation and two-stage reduction waves on CV due to the oxidation of ferrocene and the reduction of TCBD unit, respectively. We confirmed the scan rate dependency of the half-wave potentials on CV by changing the rate from 100 mVs⁻¹ to 20 mVs⁻¹, but the half-wave potentials of the electrochemical oxidation and reduction (E_1^{ox} , E_1^{red} and E_2^{red}) of TCBD chromophores **17–24** did not show any potential shifts (see Supporting Information).

Table 2. Redox potentials^[a,b] of TCBDs **17–24** bearing ferrocene substituent.

Sample	Method	E_1^{ox} [V]	E_1^{red} [V]	E_2^{red} [V]
17	CV	+0.56	-0.85	-1.16
	(DPV)	(+0.54)	(-0.83)	(-1.14)
18	CV	+0.58	-0.77	-1.09
	(DPV)	(+0.56)	(-0.75)	(-1.07)
19	CV	+0.58	-0.77	-1.06
	(DPV)	(+0.56)	(-0.75)	(-1.04)
20	CV	+0.56	-0.59	-1.03
	(DPV)	(+0.54)	(-0.57)	(-1.01)
21	CV	+0.60	-0.66	-0.97
	(DPV)	(+0.58)	(-0.64)	(-0.95)
22	CV	+0.61	-0.52	-0.79
	(DPV)	(+0.59)	(-0.50)	(-0.77)
23	CV	+0.60	-0.66	-0.96
	(DPV)	(+0.58)	(-0.64)	(-0.94)
24	CV	+0.58	-0.60	
	(DPV)	(+0.56)	(-0.58)	(-0.98)

[a] V vs. Ag/AgNO₃, 1 mM in benzonitrile containing Et₄NClO₄ (0.1 M), Pt electrode (internal diameter: 1.6 mm), scan rate = 100 mVs⁻¹, and internal reference (Fc/Fc⁺ = +0.15 V). [b] Half-wave potentials E^{ox} and $E^{\text{red}} = (E_{\text{pc}} + E_{\text{pa}})/2$ on CV, E_{pc} and E_{pa} correspond to the cathodic and anodic peak potentials, respectively.

Although the oxidation of TCBD chromophores **17** (+0.56 V) and **18** (+0.54 V) with a 1-azulenyl substituent caused at almost similar potential value on CV, the reduction potentials were affected

by the substituents on the azulene ring. Thus, the first reduction potential of **18** (-0.77 V) with electron-withdrawing methoxycarbonyl group showed a positive shift by +0.08 V compared with that of **17** (-0.85 V) with electron-donating *tert*-butyl groups (Figure 4). These results represent that the substituents on azulene ring in **17** and **18** directly exert the LUMO-level of the TCBD unit, although the HOMO is not affected by the substituents.

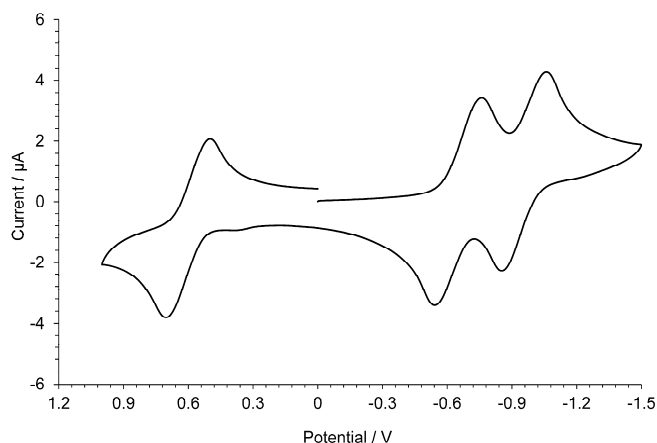


Figure 4. Cyclic voltammogram of the reduction of **17** (1 mM) in benzonitrile containing Et₄NClO₄ (0.1 M) as the supporting electrolyte; scan rate = 100 mVs⁻¹.

The electrochemical oxidation and reduction of **19** showed reversible waves at +0.58 V, -0.77 V, and -1.06 V, due to the oxidation and reduction of ferrocene and TCBD moieties, respectively. The oxidation potential of **20** (+0.56 V), which correspond to the oxidation of ferrocene unit, is almost comparable with those of **19** and TCBDs **17** and **18** with a 1-azulenyl substituent. The electrochemical reduction of **20** also exhibited a reversible two-step wave at -0.59 V and -1.03 V on CV. Positive shift of the first reduction potential of **20** by +0.18 V compared with that of **19** should be ascribed to the influence of both electron-withdrawing nature and steric hinderance of the two ethoxycarbonyl groups at the 1,3-positions.

Reversible redox waves were also observed by the electrochemical oxidation and reduction of TCBDs **21**, **22**, and **23** with a 6-azulenyl substituent on CV, which could be assumed as the formation of a cationic and dianionic species, respectively. The oxidation potentials of **21**, **22**, and **23** were identified as +0.60 V, +0.61 V, and +0.60 V by CV, respectively, due to the oxidation of the ferrocene moiety. Therefore, the HOMO-level of the ferrocene moiety was not influenced by the azulene substituent, as similar with a case of TCBDs **17–20** with a 1- or 2-azulenyl substituent. Electrochemical reduction of the TCBD **21** with a 6-azulenyl substituent showed a reversible two-stage reduction wave on CV (-0.66 V and -0.97 V) attributed to the formation up to a dianionic species. Introduction of the ethoxycarbonyl substituents to the azulene ring resulted in large shifts of the first reduction potentials as observed in the reduction of 6-azulenyl derivatives **22** and **23**. The first reduction potential of **22** (-0.52 V) with ethoxycarbonyl groups at the 1,3-positions showed positive shift by +0.14 V compared with that of **21** (Figure 5). Increment of electron affinity in **22** should be concluded to the electron-withdrawing nature of the 1,3-substituents on the azulene ring. The electrochemical reduction

of **23** also showed a reversible two-step reduction wave on CV (-0.66 V and -0.96 V) due to the formation up to a dianionic species. Despite the existence of electron-withdrawing ethoxycarbonyl groups at the 1,3-positions, the first reduction potential of **23** was observed at similar potential region with that of **21**. Thus, the 2-amino moiety of **23** increases the LUMO-level as illustrated the resonance structure in Scheme 8 by its electron-donating property. These electrochemical analyses indicate the LUMO of TCBDs can be controlled by varying substituent and substitution position on the azulene ring, with the respect to the redox potentials.

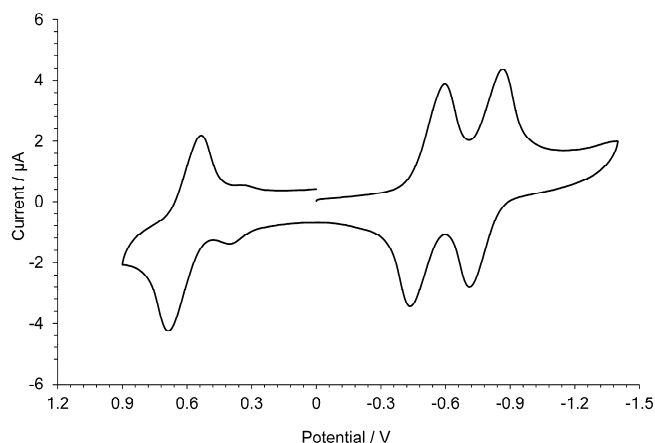
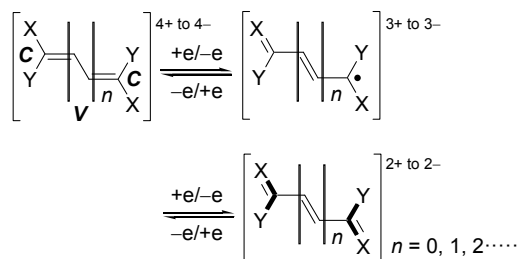


Figure 5. Cyclic voltammogram of the reduction of **22** (1 mM) in benzonitrile containing Et_4NClO_4 (0.1 M) as the supporting electrolyte; scan rate = 100 mVs^{-1} .

Electrochromism is observed in reversible redox systems that exhibit significant color changes in different oxidation states. Stabilization of the redox cycle is very important in the construction of electrochromic materials because the molecules that are utilized for this application require high redox stabilities. Hünig et al. proposed the concept of a violene–cyanine (V–C) hybrid for the production of stabilized organic electrochromic materials.^[21] The hybrid is made up of a violene-type redox system containing delocalized closed-shell polymethine (e.g., cyanine) dyes as end groups. Therefore, the redox system with the hybrid structure should provide the color of cyanine dye by an overall two-electron transfer, as illustrated in Scheme 9. The cyanine-type substructures that are generated by the two electron-transfer represented by the bold line in the general structure. Contrary to the violene-type redox system, both colored and discolored species consist of closed-shell structures. Therefore, persistency of the electrochromic system would be improved by adopting the hybrid structure.



Scheme 9. General structure of Hünig's violene–cyanine hybrid.

We have reported the synthesis of various azulene-substituted, redox-active chromophores with the aim of creating stabilized electrochromic materials.^[22] As a part of the study, we have also reported several TCBD derivatives bearing 1-azulenyl substituents, in which we have identified some novel hybrid structures of V and C with the redox activities.^[8,23] However, electrochromic properties of TCBD derivatives substituted by a 2- or 6-azulenyl group were not investigated so far. From our previous study, 2- or 6-azulenyl groups connected by π -electron systems induce electrochromic property with high reversibility, owing to the generation of stabilized anionic species. Thus, visible spectra of the new TCBDs **17–24** were monitored to clarify the color changes during the electrochemical reactions. A constant-current oxidation and reduction ($100 \mu\text{A}$) was applied to the solutions of **17–24** with a platinum mesh as the working electrode and a wire counter electrode in the electrolytic cell of 1 mm thickness.^[24] Visible spectra were measured in degassed benzonitrile containing Et_4NClO_4 (0.1 M) as a supporting electrolyte at room temperature under the electrochemical reaction conditions.

We have checked the absorption spectrum of the TCBDs **17–24** in a benzonitrile solution, because of the difference in the highly polar solvent in contrast to our spectral investigation described above. However, the TCBDs **17–24** in benzonitrile did not show significant shifts on the longest wavelength absorption bands compared with those measured in dichloromethane (see Supporting Information). Thus, we utilize benzonitrile as a solvent for the electrochemical studies because of its advantage in the electrochromic study.

We expected the reversible color change of **17–24** under electrochemical oxidation conditions owing to the generation of ferrocenium ion. However, reversibility could not be observed by the electrochromic study of **17–24** under the conditions of the spectral measurements. These results might be concluded the destabilization of the generated ferrocenium ion by the electrochemical oxidation owing to the electron-withdrawing TCBD moiety (see Supporting Information). The longest absorption of **17** at around 500 nm gradually decreased during the electrochemical reduction, along with the development of a new absorption in the visible region at 710 nm, which spread into near-infrared region. The color change from red to pale yellow of the solution was detectable during the electrochemical reduction. However, reverse oxidation of the pale yellow solution did not regenerate the original spectrum of **17**. When the visible spectral changes of **18** were measured under similar reduction conditions, absorption of **18** at around 460 nm gradually decreased, together with the generation of new absorptions at 540 nm and 680 nm. Reverse oxidation decreased the new absorptions, but did not regenerate the original absorption of **18**, completely. Poor reversibility for the color changes of **17** and **18** should be attributable to the instability of the presumed dianionic species under the conditions of the spectral measurements, due to the electron-donating nature of 1-azulenyl and ferrocenyl moieties substituted.

In contrast to the results on **17** and **18**, color changes of TCBDs **19–23** bearing a 2- or 6-azulenyl substituent were observed with higher reversibility. When the spectral changes of TCBD **19** with a 2-azulenyl substituent were monitored during the electrochemical reduction, new absorption at 530 nm spread into near-infrared region gradually developed, together with the color change from pale green to purple. Reverse oxidation caused decrease of the new

absorptions and regenerated the original color of **19** (Figure 6). When the UV–visible spectra of **20** were measured under electrochemical reduction conditions, the absorption in the visible region gradually decreased and new absorptions in the visible region at around 540 nm and 680 nm, which spread into near-infrared region, were gradually developed. Reverse oxidation decreased the new absorptions, along with the color change from purple to the original pale green color.

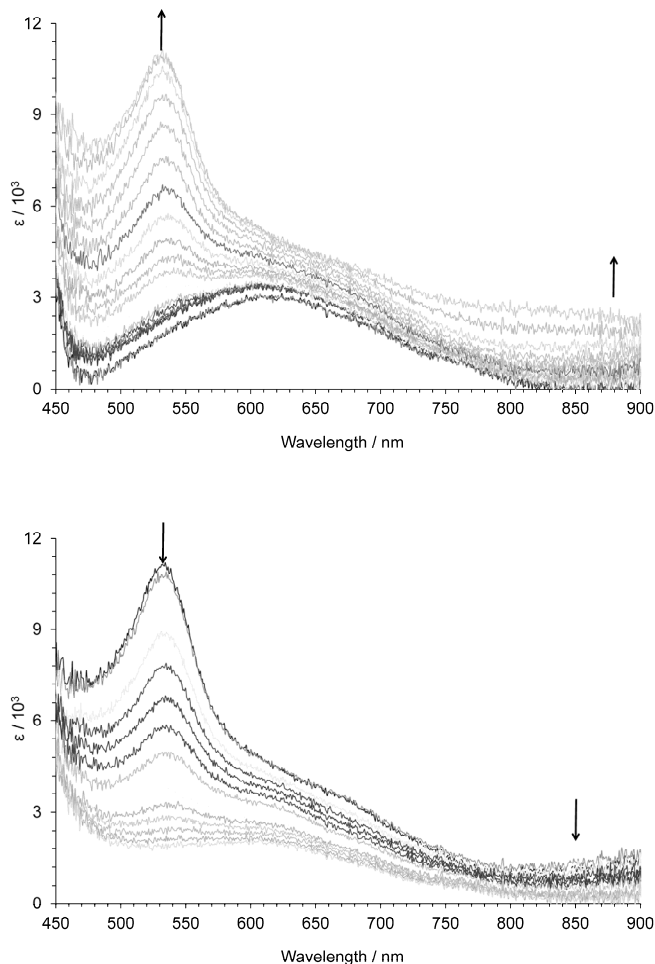


Figure 6. Continuous change in the UV/Vis spectra of **19**: constant-current electrochemical reduction (100 μ A, top) and reverse oxidation of the reduced species (100 μ A, bottom) in benzonitrile containing Et_4NClO_4 (0.1 M) at 30 sec intervals.

Two absorption bands at around 520 nm and 650 nm spread into near-infrared region were generated on the spectral change of **21** under the electrochemical reduction conditions. The color of the solution of **21** gradually changed from greenish blue to yellow during the electrochemical reduction. The color change could be ascribed to the formation of a dianionic species in the two-electron reduction. A reversible color change was also observed in the visible spectral changes of **22** under the electrochemical reduction conditions (Figure 7). The electrochemical reduction gradually developed new absorptions in the visible region at 510 nm and 610 nm spread into near-infrared region and the greenish-blue color of the solution was changed to yellow. Reverse oxidation decreased the new absorptions in near-infrared region and regenerated the original absorption of **22** in the visible region. When the spectral changes of **23** were monitored during the electrochemical reduction, the absorption in the visible region gradually decreased with the

development of new, broad absorptions, spread into near-infrared region, at around 640 nm and 870 nm. Reverse oxidation decreased the new absorptions and regenerated the original reddish-purple color of the solution of **23**. UV/Vis spectra of **24** were also measured under the electrochemical reduction conditions, the absorption bands of **24** at around 450 nm to 650 nm also gradually increased. However, reverse oxidation of the solution did not regenerate the original spectra of **24**.

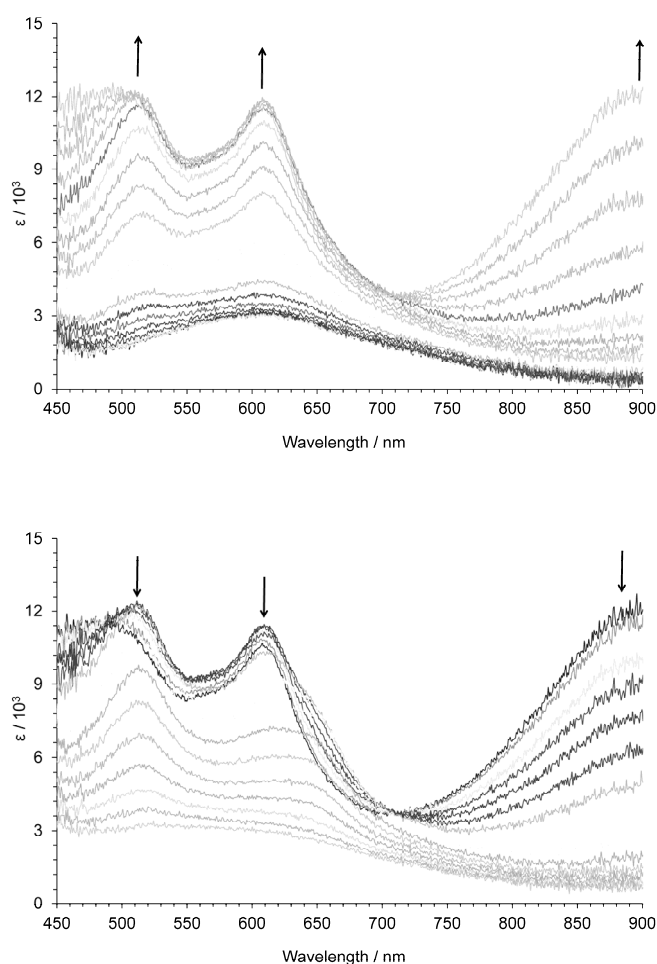


Figure 7. Continuous change in the UV/Vis spectrum of **22**: constant-current electrochemical reduction (100 μ A, top) and reverse oxidation of the reduced species (100 μ A, bottom) in benzonitrile containing Et_4NClO_4 (0.1 M) at 30 sec intervals.

From the results described above, the new TCBD derivatives substituted by a 2- or 6-azulenyl group were revealed to display certain reversibility under the electrochemical conditions with significant color changes, although the ferrocene-substituted TCBD **24** showed poor reversibility. We have reported the synthesis of various azulene-substituted redox-active chromophores with the aim of creating stabilized electrochromic materials. In these studies, we have revealed that TCBD derivatives combined with a 2- or 6-azulenyl group as a terminal group provide stabilized electrochromic materials exhibiting strong absorptions spread into near-infrared region in their two-electron reduced state. Electrochromic behavior with higher reversibility in TCBD derivatives substituted by a 2- or 6-azulenyl group should be ascribed to the stabilization of anionic species by the substituted azulene ring.

Conclusion

(Ferrocenylethynyl)azulenes **10–16** were prepared by palladium-catalyzed Sonogashira–Hagihara reaction. A series of TCBD chromophores **17–23** bearing both azulene and ferrocene substituents were synthesized in a one-step procedure consisting of the formal [2+2] cycloaddition reaction of **10–16** with TCNE, followed by the ring-opening reaction of the initially formed cyclobutene derivatives. Intramolecular CT absorption bands were found in the UV–visible spectra of TCBD chromophores **17–23**. An analysis by CV and DPV showed that TCBDs **17–23** exhibited a reversible two-stage reduction wave, as well as reversible one-stage oxidation wave. Moreover, a significant color changes were observed during the electrochemical reduction. In particular, TCBDs **19–23** bearing a 2- or 6-azulenyl substituent exhibited color changes with higher reversibility, attributable to the stabilization of anionic species during the electrochemical reaction. These results showed that TCBDs **19–23** behaved like a V–C hybrid, a concept proposed by Hünig and his co-workers, in view of the formation of the stabilized dianionic species by the two-electron reduction.

These results would warrant the use of these donor–acceptor systems as organic electronic and optoelectronic materials. To evaluate the scope of this class of molecules investigated by this research, the preparation of novel azulene-substituted TCBD chromophores connected with various π -electron cores is now in progress in our laboratory.

Experimental Section

General: Melting points were determined with a Yanagimoto MPS3 micro melting apparatus and are uncorrected. Mass spectra were obtained with Bruker APEX II instruments. IR and UV/Vis spectra were measured with JASCO FT/IR-4100 and Shimadzu UV-2550 spectrophotometers, respectively. ^1H and ^{13}C NMR spectra were recorded with a JEOL ECA-500 spectrometer (at 500 MHz and 125 MHz, respectively), or a JEOL ECA-600 spectrometer (at 600 MHz and 150 MHz, respectively). Gel permeation chromatography (GPC) purification was performed with a TSKgel G2000H₈ with CHCl₃ or Bio-Beads with CH₂Cl₂ as an eluent. Voltammetry measurements were carried out with a BAS 100B/W electrochemical workstation equipped with Pt working and auxiliary electrodes and a reference electrode formed from Ag/AgNO₃ (0.01 M) in acetonitrile containing tetrabutylammonium perchlorate (0.1 M). Elemental analyses were performed at the Research and Analytical Center for Giant Molecules, Graduate School of Science, Tohoku University.

1,1,4,4-Tetracyano-2-(1,6-di-tert-butylazulen-3-yl)-3-ferrocenyl-1,3-butadiene (17): To a solution of **10** (224 mg, 0.50 mmol) in ethyl acetate (5 mL) was added TCNE (96 mg, 0.75 mmol). The resulting mixture was stirred at room temperature for 1 h under an Ar atmosphere. The solvent was removed under reduced pressure. The residue was purified by column chromatography on silica gel with ethyl acetate and Bio-Beads with CH₂Cl₂ to give **17** (265 mg, 92%) as purple crystals. M.p. 190.0 – 195.0 °C (AcOEt); IR (KBr disk): ν_{max} = 3103 (w), 2966 (m), 2870 (w), 2208 (s), 2218 (s), 1579 (m), 1512 (s), 1469 (s), 1433 (s), 1415 (s), 1396 (m), 1375 (s), 1365 (s), 1358 (s), 1325 (m), 1294 (m), 1279 (m), 1257 (m), 1217 (m), 1109 (m), 1095 (m), 1076 (w), 1049 (w), 1005 (w), 951 (w), 873 (w), 841 (w), 825 (w), 812 (w), 775 (w), 736 (w), 679 (w), 659 (w), 628 (w), 609 (w), 503 (w), 480 (w), 445 (w) cm^{-1} ; UV/Vis (CH₂Cl₂): λ_{max} (log ϵ) = 248 (4.48), 298 (4.33), 342 (4.36), 426 (3.92), 492 (4.16), 590 sh (3.62) nm; UV/Vis (10% CH₂Cl₂/hexane): λ_{max} (log ϵ) = 245 (4.47), 297 (4.33), 342 (4.33), 413 sh (3.88), 484 (4.20), 590 sh (3.62) nm; UV/Vis (benzonitrile): λ_{max} (log ϵ) = 347 (4.35), 417 (4.15), 485 (4.16), 590 sh (3.78) nm; ^1H NMR (500 MHz, CDCl₃): δ_{H} = 8.81 (d, 1H, J = 10.0 Hz, H₄), 8.31 (d, 1H, J = 10.0 Hz, H₈), 7.92 (d, 1H, J = 10.0 Hz, H₅), 7.84 (d, 1H, J = 10.0 Hz, H₇), 7.49 (s, 1H, H₂), 5.23 (s, 1H, H of ferrocene), 4.94 (s, 1H, H of ferrocene), 4.83 (s, 2H, H of ferrocene), 4.43 (s, 5H, Cp), 1.52 (s, 9H, *t*Bu), 1.51 (s, 9H, *i*Bu) ppm; $^{13}\text{C}\{^1\text{H}\}$ NMR (125 MHz, CDCl₃): δ_{C} = 175.35, 166.38, 158.96, 143.01, 142.98, 140.41, 137.54, 136.68, 135.19, 127.98, 127.64, 118.60, 114.69, 114.12, 113.95, 113.15, 78.75, 76.39, 75.72, 75.18, 74.58, 72.25, 71.95, 71.88, 39.08, 33.09, 31.68, 31.35 ppm; HRMS (ESI): Calcd for C₃₆H₃₂N₄Fe + Na⁺ [M + Na]⁺ 599.1874. Found: 599.1869; Anal. Calcd for C₃₆H₃₂N₄Fe·2/5H₂O: C, 74.07; H, 5.66; N, 9.60. Found: C, 73.98; H, 5.51; N, 9.57.

1,1,4,4-Tetracyano-2-ferrocenyl-3-(7-isopropyl-1-methoxycarbonylazulen-3-yl)-1,3-butadiene (18): To a solution of **11** (218 mg, 0.50 mmol) in ethyl acetate (5 mL) was

added TCNE (96 mg, 0.75 mmol). The resulting mixture was stirred at room temperature for 2 h under an Ar atmosphere. The solvent was removed under reduced pressure. The residue was purified by column chromatography on silica gel with ethyl acetate and Bio-Beads with CH₂Cl₂ to give **18** (273 mg, 97%) as red crystals. M.p. 115.0 – 118.0 °C (AcOEt/hexane); IR (KBr disk): ν_{max} = 2952 (w), 2220 (w), 1698 (m), 1499 (s), 1441 (s), 1418 (s), 1364 (m), 1319 (w), 1285 (w), 1239 (m), 1213 (s), 1178 (m), 1126 (w), 1050 (w), 895 (w), 820 (w), 768 (w), 753 (m), 666 (w), 635 (w), 603 (w) cm^{-1} ; UV/Vis (CH₂Cl₂): λ_{max} (log ϵ) = 261 (4.40), 301 (4.40), 342 (4.30), 389 sh (3.99), 459 (4.10), 644 sh (3.31) nm; UV/Vis (10% CH₂Cl₂/hexane): λ_{max} (log ϵ) = 260 (4.47), 300 (4.47), 339 (4.38), 391 (4.00), 451 (4.21), 547 sh (3.54), 597 sh (3.52) nm; UV/Vis (benzonitrile): λ_{max} (log ϵ) = 334 sh (4.31), 394 sh (4.24), 412 (4.26), 447 sh (4.21) nm; ^1H NMR (500 MHz, CDCl₃): δ_{H} = 9.97 (s, 1H, H₈), 8.46 (d, 1H, J = 10.0 Hz, H₄), 8.32 (s, 1H, H₂), 8.14 (d, 1H, J = 10.0 Hz, H₆), 7.98 (dd, 1H, J = 10.0 Hz, H₅), 5.12 (s, 1H, H of ferrocene), 5.02 (s, 1H, H of ferrocene), 4.98 (s, 1H, H of ferrocene), 4.92 (s, 1H, H of ferrocene), 4.50 (s, 5H, Cp), 3.95 (s, 3H, CO₂Me), 3.35 (sept, 1H, J = 6.9 Hz, *i*Pr), 1.47 (d, 6H, J = 6.9 Hz, *i*Pr) ppm; $^{13}\text{C}\{^1\text{H}\}$ NMR (125 MHz, CDCl₃): δ_{C} = 175.00 (C=C(CN)₂), 164.46 (CO₂Me), 160.93 (C=C(CN)₂), 156.38 (C₇), 145.93 (C_{3a}), 142.38 (C₂), 142.26 (C₆), 141.32 (C_{8a}), 140.56 (C₈), 137.57 (C_a), 131.87 (C₅), 118.58 (C₁), 118.54 (C₃), 113.90 (CN), 113.55 (CN), 113.10 (CN), 112.76 (CN), 80.17 (C(CN)₂), 78.89 (C(CN)₂), 75.97 (C of ferrocene), 75.37 (C of ferrocene), 75.11 (C of ferrocene), 72.46 (Cp), 72.08 (C of ferrocene), 51.66 (CO₂Me), 39.46 (*i*Pr), 24.50 (*i*Pr) ppm; The one signal of ferrocene moiety was overlapped with CDCl₃. HRMS (FAB): Calcd for C₃₃H₂₄N₄O₂Fe + H⁺ [M + H]⁺ 565.1327. Found: 565.1317; Anal. Calcd for C₃₃H₂₄N₄O₂Fe: C, 70.22; H, 4.29; N, 9.93. Found: C, 70.02; H, 4.52; N, 9.89.

2-(2-Azulenyl)-1,1,4,4-tetracyano-3-ferrocenyl-1,3-butadiene (19): To a solution of **12** (168 mg, 0.50 mmol) in ethyl acetate (5 mL) was added TCNE (96 mg, 0.75 mmol). The resulting mixture was stirred at room temperature for 3 h under an Ar atmosphere. The solvent was removed under reduced pressure. The residue was purified by column chromatography on silica gel with ethyl acetate and Bio-Beads with CH₂Cl₂ to give **19** (216 mg, 93%) as reddish-blue crystals. M.p. 238.0 – 240.0 °C (AcOEt/hexane); IR (KBr disk): ν_{max} = 3117 (w), 3092 (w), 2220 (m), 2212 (m), 1578 (w), 1551 (m), 1535 (m), 1520 (s), 1483 (w), 1466 (m), 1439 (m), 1400 (w), 1379 (w), 1340 (m), 1319 (m), 1294 (w), 1280 (w), 1228 (m), 1217 (m), 1159 (w), 1111 (w), 1088 (w), 1069 (w), 1051 (w), 1026 (w), 1005 (w), 985 (w), 968 (w), 935 (w), 893 (w), 860 (w), 825 (w), 817 (w), 760 (w), 740 (w), 696 (w), 663 (w), 615 (w), 605 (w), 574 (w), 530 (w), 508 (w), 495 (w), 486 (w), 449 (w), 401 (w) cm^{-1} ; UV/Vis (CH₂Cl₂): λ_{max} (log ϵ) = 252 (4.51), 316 (4.61), 402 (4.41), 427 sh (4.17), 616 (3.48) nm; UV/Vis (10% CH₂Cl₂/hexane): λ_{max} (log ϵ) = 253 (4.51), 318 (4.64), 380 sh (4.32), 399 (4.38), 420 sh (4.10), 590 (3.43) nm; UV/Vis (benzonitrile): λ_{max} (log ϵ) = 322 (4.60), 405 (4.49), 610 (3.44) nm; ^1H NMR (500 MHz, CDCl₃): δ_{H} = 8.37 (d, 2H, J = 10.0 Hz, H_{4,8}), 7.73 (t, 1H, J = 10.0 Hz, H₆), 7.64 (s, 2H, H_{1,3}), 7.25 (t, 2H, J = 10.0 Hz, H_{5,7}), 5.47 (br s, 1H, H of ferrocene), 4.99 (br s, 1H, H of ferrocene), 4.78 (br s, 1H, H of ferrocene), 4.52 (br s, 1H, H of ferrocene), 4.45 (s, 5H, Cp) ppm; $^{13}\text{C}\{^1\text{H}\}$ NMR (125 MHz, CDCl₃): δ_{C} = 173.14 (C=C(CN)₂), 160.93 (C=C(CN)₂), 143.08 (C₆), 142.68 (C_{4,8}), 140.55 (C_{3a,8a}), 136.60 (C₂), 125.88 (C_{5,7}), 118.92 (C_{1,3}), 113.83 (CN), 113.01 (CN), 112.82 (CN), 112.47 (CN), 82.64 (C(CN)₂), 78.61 (C(CN)₂), 75.94 (C of ferrocene), 75.54 (C of ferrocene), 74.67 (C of ferrocene), 72.51 (Cp), 72.00 (C of ferrocene), 71.91 (C of ferrocene) ppm; HRMS (ESI): Calcd for C₂₈H₁₆N₄Fe + Na⁺ [M + Na]⁺ 487.0622. Found: 487.0617; Anal. Calcd for C₂₈H₁₆N₄Fe: C, 72.43; H, 3.47; N, 12.07. Found: C, 72.13; H, 3.62; N, 12.05.

1,1,4,4-Tetracyano-2-(1,3-diethoxycarbonylazulen-2-yl)-3-ferrocenyl-1,3-butadiene (20): To a solution of **13** (240 mg, 0.50 mmol) in ethyl acetate (5 mL) was added TCNE (96 mg, 0.75 mmol). The resulting mixture was refluxed for 6 h under an Ar atmosphere. The solvent was removed under reduced pressure. The residue was purified by column chromatography on silica gel with ethyl acetate and Bio-Beads with CH₂Cl₂ to give **20** (271 mg, 89%) as reddish-brown crystals. M.p. 162.0 – 164.0 °C (AcOEt/hexane); IR (KBr disk): ν_{max} = 3069 (w), 2973 (w), 2223 (w), 1701 (m), 1693 (m), 1562 (w), 1537 (w), 1523 (m), 1449 (m), 1403 (w), 1381 (w), 1320 (w), 1292 (w), 1260 (w), 1210 (s), 1110 (w), 1057 (w), 1018 (m), 913 (w), 838 (w), 768 (w), 739 (w), 676 (w), 629 (w) cm^{-1} ; UV/Vis (CH₂Cl₂): λ_{max} (log ϵ) = 234 (4.51), 307 (4.68), 360 sh (4.24), 387 sh (4.06), 556 (3.24), 753 (3.07) nm; UV/Vis (10% CH₂Cl₂/hexane): λ_{max} (log ϵ) = 306 (4.71), 363 sh (4.25), 553 (3.28), 724 (3.14) nm; UV/Vis (benzonitrile): λ_{max} (log ϵ) = 309 (4.65), 362 sh (4.25), 388 sh (4.09), 556 (3.24), 753 (3.07) nm; ^1H NMR (500 MHz, CDCl₃, 55 °C): δ_{H} = 9.81 (d, 2H, J = 10.0 Hz, H_{4,8}), 8.07 (t, 1H, J = 10.0 Hz, H₆), 7.79 (t, 2H, J = 10.9 Hz, H_{5,7}), 5.29 (br s, 2H, H of ferrocene), 4.75 (br s, 2H, H of ferrocene), 4.56 (q, 4H, J = 7.5 Hz, CO₂Et), 4.43 (s, 5H, Cp), 1.51 (t, 6H, J = 7.5 Hz, CO₂Et) ppm; $^{13}\text{C}\{^1\text{H}\}$ NMR (125 MHz, CDCl₃, 55 °C): δ_{C} = 170.12 (C=C(CN)₂), 164.02 (CO₂Et), 162.46 (C=C(CN)₂), 144.00 (C₆), 142.56 (C_{4,8}), 141.55 (C_{3a,8a}), 131.58 (C_{5,7}), 115.23 (C_{1,3}), 113.63 (CN), 112.44 (CN), 111.58 (CN), 108.65 (CN), 94.40 (C(CN)₂), 81.93 (C(CN)₂), 74.18 (C_{2,3,4,5} of ferrocene), 72.11 (Cp), 70.10 (C₁ of ferrocene), 61.80 (CO₂Et), 14.46 (CO₂Et) ppm; HRMS (FAB): Calcd for C₃₄H₂₄N₄O₄Fe⁺ [M]⁺ 608.1147. Found: 608.1150; Anal. Calcd for C₃₄H₂₄N₄O₄Fe: C, 67.12; H, 3.98; N, 9.21. Found: C, 67.02; H, 3.99; N, 9.20.

2-(6-Azulenyl)-1,1,4,4-tetracyano-3-ferrocenyl-1,3-butadiene (21): To a solution of **14** (168 mg, 0.50 mmol) in ethyl acetate (5 mL) was added TCNE (96 mg, 0.75 mmol). The resulting mixture was refluxed for 30 min under an Ar atmosphere. The solvent was removed under reduced pressure. The residue was purified by column chromatography

on silica gel with ethyl acetate and Bio-Beads with CH₂Cl₂ to give **21** (211 mg, 91%) as blue crystals. M.p. > 300 °C (AcOEt); IR (KBr disk): ν_{\max} = 3094 (w), 2220 (s), 1578 (w), 1540 (w), 1510 (s), 1477 (m), 1442 (s), 1412 (m), 1396 (m), 1383 (m), 1354 (m), 1329 (m), 1300 (m), 1277 (w), 1257 (m), 1234 (m), 1196 (w), 1163 (m), 1109 (m), 1084 (w), 1064 (w), 1051 (m), 1037 (m), 1003 (m), 992 (m), 937 (w), 908 (w), 893 (w), 881 (w), 846 (s), 829 (s), 789 (w), 767 (s), 719 (w), 679 (m), 671 (m), 630 (w), 609 (w), 561 (w), 540 (m), 505 (m), 486 (s), 457 (w), 420 (w) cm⁻¹; UV/Vis (CH₂Cl₂): λ_{\max} (log ϵ) = 258 (4.43), 296 (4.67), 316 sh (4.53), 394 sh (4.06), 638 (3.43) nm; UV/Vis (10% CH₂Cl₂/hexane): λ_{\max} (log ϵ) = 260 (4.45), 295 (4.72), 314 sh (4.59), 385 sh (4.07), 620 (3.42) nm; UV/Vis (benzonitrile): λ_{\max} (log ϵ) = 316 sh (4.53), 392 sh (4.12), 634 (3.43) nm; ¹H NMR (500 MHz, CDCl₃): δ_{H} = 8.39 (d, 2H, J = 10.0 Hz, H_{4,8}), 8.12 (br s, 1H, H₂), 7.54 (d, 2H, J = 4.0 Hz, H_{1,3}), 7.61 (br s, 2H, H_{5,7}), 5.33 (br s, 1H, H of ferrocene), 4.97 (br s, 1H, H of ferrocene), 4.84 (br s, 1H, H of ferrocene), 4.74 (br s, 1H, H of ferrocene), 4.40 (s, 5H, Cp) ppm; ¹³C{¹H} NMR (125 MHz, CDCl₃): δ_{C} = 172.08 (C=C(CN)₂), 170.19 (C=C(CN)₂), 142.46 (C₂), 141.00 (C_{3a,8a}), 138.63 (C₆), 135.03 (C_{4,8}), 121.65 (C_{5,7}), 121.48 (C_{1,3}), 113.76 (CN), 113.22 (CN), 111.47 (CN), 111.16 (CN), 89.64 (C(CN)₂), 79.29 (C(CN)₂), 75.86 (C of ferrocene), 75.04 (C of ferrocene), 74.84 (C of ferrocene), 72.85 (C of ferrocene), 72.66 (Cp), 71.39 (C₁ of ferrocene) ppm; HRMS (ESI): Calcd for C₂₈H₁₆N₄Fe + Na⁺ [M + Na]⁺ 487.0622. Found: 487.0617; Anal. Calcd for C₂₈H₁₆N₄Fe·1/2H₂O: C, 70.82; H, 3.50; N, 11.81. Found: C, 71.05; H, 3.62; N, 11.84.

1,1,4,4-Tetracyano-2-(1,3-dithoxycarbonylazulen-6-yl)-3-ferrocenyl-1,3-butadiene (**22**):

To a solution of **15** (240 mg, 0.50 mmol) in ethyl acetate (5 mL) was added TCNE (96 mg, 0.75 mmol). The resulting mixture was refluxed for 2 h under an Ar atmosphere. The solvent was removed under reduced pressure. The residue was purified by column chromatography on silica gel with ethyl acetate and Bio-Beads with CH₂Cl₂ to give **22** (268 mg, 88%) as red crystals. M.p. 159.0 – 162.0 °C (AcOEt/hexane); IR (KBr disk): ν_{\max} = 2980 (w), 2221 (w), 1698 (m), 1517 (m), 1437 (s), 1388 (w), 1292 (w), 1246 (w), 1206 (s), 1052 (w), 1040 (m), 1035 (m), 984 (w), 921 (w), 823 (w), 769 (w), 647 (w), 606 (w) cm⁻¹; UV/Vis (CH₂Cl₂): λ_{\max} (log ϵ) = 249 (4.55), 314 sh (4.60), 335 (4.67), 380 sh (4.28), 621 (3.47) nm; UV/Vis (10% CH₂Cl₂/hexane): λ_{\max} (log ϵ) = 247 (4.63), 310 sh (4.67), 332 (4.75), 378 sh (4.28), 603 (3.52) nm; UV/Vis (benzonitrile): λ_{\max} (log ϵ) = 316 sh (4.55), 338 (4.61), 379 sh (4.27), 616 (3.49) nm; ¹H NMR (500 MHz, CDCl₃): δ_{H} = 9.81 (d, 2H, J = 10.9 Hz, H_{4,8}), 8.99 (s, 1H, H₂), 7.72 (d, 2H, J = 10.9 Hz, H_{5,7}), 5.45 (br s, 1H, H of ferrocene), 5.05 (br s, 1H, H of ferrocene), 4.90 (br s, 1H, H of ferrocene), 4.63 (br s, 1H, H of ferrocene), 4.45 (q, 4H, J = 7.5 Hz, CO₂Et), 4.44 (s, 5H, Cp), 1.46 (t, 6H, J = 7.5 Hz, CO₂Et) ppm; ¹³C{¹H} NMR (125 MHz, CDCl₃): δ_{C} = 171.42 (C=C(CN)₂), 168.24 (C=C(CN)₂), 164.10 (CO₂Et), 147.34 (C₂), 143.86 (C_{3a,8a}), 141.42 (C₆), 137.95 (C_{4,8}), 128.36 (C_{5,7}), 119.04 (C_{1,3}), 113.49 (CN), 113.16 (CN), 110.97 (CN), 110.57 (CN), 90.92 (C(CN)₂), 79.00 (C(CN)₂), 76.49 (C of ferrocene), 75.41 (C of ferrocene), 74.32 (C of ferrocene), 73.32 (C of ferrocene), 72.92 (Cp), 71.08 (C of ferrocene), 60.70 (CO₂Et), 14.50 (CO₂Et) ppm; HRMS (FAB): Calcd for C₃₄H₂₄N₄O₄Fe⁺ [M]⁺ 608.1147. Found: 608.1150; Anal. Calcd for C₃₄H₂₄N₄O₄Fe: C, 67.12; H, 3.98; N, 9.21. Found: C, 67.01; H, 4.03; N, 9.18.

2-(2-Amino-1,3-dithoxycarbonylazulen-6-yl)-1,1,4,4-tetracyano-3-ferrocenyl-1,3-butadiene (**23**):

To a solution of **16** (248 mg, 0.50 mmol) in ethyl acetate (5 mL) was added TCNE (96 mg, 0.75 mmol). The resulting mixture was refluxed for 1 h under an Ar atmosphere. The solvent was removed under reduced pressure. The residue was purified by column chromatography on silica gel with ethyl acetate and Bio-Beads with CH₂Cl₂ to give **23** (290 mg, 93%) as reddish-brown crystals. M.p. > 300.0 °C (AcOEt); IR (KBr disk): ν_{\max} = 3366 (w), 2224 (w), 1691 (m), 1605 (m), 1577 (m), 1521 (m), 1510 (s), 1442 (m), 1386 (w), 1329 (w), 1281 (m), 1252 (w), 1153 (m), 1143 (m), 1111 (m), 1093 (m), 1067 (w), 1022 (m), 943 (m), 831 (w), 805 (w), 787 (w), 691 (m) cm⁻¹; UV/Vis (CH₂Cl₂): λ_{\max} (log ϵ) = 246 (4.56), 295 sh (4.34), 343 (4.67), 408 sh (4.04), 499 (4.28), 640 sh (3.38) nm; UV/Vis (10% CH₂Cl₂/hexane): λ_{\max} (log ϵ) = 244 (4.57), 291 sh (4.33), 341 (4.70), 380 sh (4.16), 406 sh (4.02), 492 (4.32), 616 sh (3.37) nm; UV/Vis (benzonitrile): λ_{\max} (log ϵ) = 347 (4.67), 362 sh (4.25), 388 sh (4.09), 556 (3.24), 753 (3.07) nm; ¹H NMR (500 MHz, CDCl₃): δ_{H} = 9.02 (d, 2H, J = 9.5 Hz, H_{4,8}), 8.28 (s, 2H, NH₂), 7.61 (d, 2H, J = 9.5 Hz, H_{5,7}), 5.30 (br s, 1H, H of ferrocene), 5.00 (br s, 1H, H of ferrocene), 4.87 (br s, 1H, H of ferrocene), 4.72 (br s, 1H, H of ferrocene), 4.48 (q, 4H, J = 6.5 Hz, CO₂Et), 4.43 (s, 5H, Cp), 1.49 (t, 6H, J = 6.5 Hz, CO₂Et) ppm; ¹³C{¹H} NMR (125 MHz, CDCl₃): δ_{C} = 172.58 (C=C(CN)₂), 168.70 (C=C(CN)₂), 165.82 (CO₂Et), 165.04 (C₂), 146.73 (C_{3a,8a}), 132.82 (C₆), 131.29 (C_{5,7}), 128.37 (C_{4,8}), 113.76 (CN), 113.13 (CN), 111.80 (CN), 111.70 (CN), 102.73 (C_{1,3}), 86.83 (C(CN)₂), 79.09 (C(CN)₂), 75.93 (C of ferrocene), 75.26 (C of ferrocene), 75.03 (C of ferrocene), 72.61 (Cp), 71.81 (C₁ of ferrocene), 60.69 (CO₂Et), 14.64 (CO₂Et) ppm; The one signal of ferrocene moiety was overlapped with CDCl₃. HRMS (FAB): Calcd for C₃₄H₂₅N₅O₄Fe + H⁺ [M + H]⁺ 624.1334. Found: 624.1335; Anal. Calcd for C₃₄H₂₅N₅O₄Fe: C, 65.50; H, 4.04; N, 11.23. Found: C, 65.37; H, 4.15; N, 11.19.

Acknowledgements

This work was partially supported by a Grant-in-Aid for Research Activity Start-up (Grant 22850007 to T.S.) from the Ministry of Education, Culture, Sports, Science, and Technology, Japan. We are grateful to Dr. Hirosuke Tatsumi of Shinshu University for valuable comments on this study.

- [1] a) K. Deuchert, S. Hünig, *Angew. Chem., Int. Ed.* **1978**, *17*, 875–886; b) M. B. Nielsen, F. Diederich, *Chem. Rev.* **2005**, *105*, 1837–1867.
- [2] a) P. L. Pauson, *Rev. Chem. Soc.* **1955**, *9*, 391–414; b) H. Nishihara, *Adv. Inorg. Chem.* **2002**, *53*, 41–86; c) D. R. VanStaveren, N. M. Nolte, *Chem. Rev.* **2004**, *104*, 5931–5985; d) R. C. J. Atkinson, V. C. Gibson, N. J. Long, *Chem. Soc. Rev.* **2004**, *33*, 313–328; e) S. I. Kirin, H. B. Kraatz, N. M. Nolte, *Chem. Soc. Rev.* **2006**, *35*, 348–354.
- [3] T. Mochida, S. Yamazaki, *J. Chem. Soc., Dalton Trans.* **2002**, 3559–3564.
- [4] a) S. Kato, M. Kivala, W. B. Schweizer, C. Boudon, J.-P. Gisselbrecht, F. Diederich, *Chem. Eur. J.* **2009**, *15*, 8687–8691; b) M. Jordan, M. Kivala, C. Boudon, J.-P. Gisselbrecht, W. B. Schweizer, P. Seiler, F. Diederich, *Chem. Asian J.* **2011**, *6*, 396–401.
- [5] T. Michinobu, *Pure Appl. Chem.* **2010**, *82*, 1001–1009.
- [6] K.-P. Zeller, *Azulene in Methoden Org. Chem. (Houben-Weyl)* 4th ed. **1952**, Vol. V, Part 2c, 1985, pp. 127–418.
- [7] a) S. Ito, N. Morita, T. Asao, *J. Org. Chem.* **1996**, *61*, 5077–5082; b) T. Shoji, J. Higashi, S. Ito, K. Toyota, T. Iwamoto, N. Morita, *Eur. J. Org. Chem.* **2009**, 5948–5952; c) T. Shoji, J. Higashi, S. Ito, N. Morita, *Eur. J. Inorg. Chem.* **2010**, 4886–4891.
- [8] T. Shoji, S. Ito, K. Toyota, M. Yasunami, N. Morita, *Chem. Eur. J.* **2008**, *14*, 8398–8408.
- [9] a) S. Ito, H. Inabe, T. Okujima, N. Morita, M. Watanabe, N. Harada, K. Imafuku, *J. Org. Chem.* **2001**, *66*, 7090–7101; b) S. Ito, A. Nomura, N. Morita, C. Kabuto, H. Kobayashi, S. Maejima, K. Fujimori, M. Yasunami, *J. Org. Chem.* **2002**, *67*, 7295–7302; c) S. Ito, T. Okujima, N. Morita, *J. Chem. Soc. Perkin Trans. 1* **2002**, 1896–1905; d) S. Ito, H. Inabe, N. Morita, K. Ohta, T. Kitamura, K. Imafuku, *J. Am. Chem. Soc.* **2003**, *125*, 1669–1680; e) S. Ito, T. Kubo, N. Morita, T. Ikoma, S. Tero-Kubota, A. Tajiri, *J. Org. Chem.* **2003**, *68*, 9753–9762; f) S. Ito, H. Inabe, N. Morita, A. Tajiri, *Eur. J. Org. Chem.* **2004**, 1774–1780; g) S. Ito, T. Kubo, N. Morita, T. Ikoma, S. Tero-Kubota, J. Kawakami, A. Tajiri, *J. Org. Chem.* **2005**, *70*, 2285–2293; h) S. Ito, T. Iida, J. Kawakami, T. Okujima, N. Morita, *Eur. J. Org. Chem.* **2009**, 5355–5364.
- [10] a) T. Yamamoto, K. Toyota, N. Morita, *Tetrahedron Lett.* **2010**, *51*, 1364–1366; b) T. Shoji, J. Higashi, S. Ito, T. Okujima, M. Yasunami, N. Morita, *Chem. Eur. J.* **2011**, *17*, 5116–5129.
- [11] a) S. Ito, N. Morita, T. Asao, *Bull. Chem. Soc. Jpn.* **1995**, *68*, 1409–1436; b) T. Shoji, S. Ito, T. Okujima, J. Higashi, R. Yokoyama, K. Toyota, M. Yasunami, N. Morita, *Eur. J. Org. Chem.* **2009**, 1554–1563.
- [12] M. Yasunami, S. Miyoshi, N. Kanegae, K. Takase, *Bull. Chem. Soc. Jpn.* **1993**, *66*, 892–899.
- [13] a) K. Sonogashira, Y. Tohda, N. Hagihara, *Tetrahedron Lett.* **1975**, *16*, 4467–4470; b) S. Takahashi, Y. Kuroyama, K. Sonogashira, N. Hagihara, *Synthesis* **1980**, 627–630; c) K. Sonogashira, Coupling reactions between sp² and sp carbon centers, in *Comprehensive Organic Synthesis*, vol. 3 (Eds.: B. M. Trost, I. Fleming), Pergamon, Oxford, **1991**, chapter 2.4, p. 521–549; d) K. Sonogashira Cross-coupling reactions to sp carbon atoms, in *Metal-Catalyzed Cross-Coupling Reactions* (Eds.: F. Diederich, P. J. Stang), Wiley-VCH, Weinheim, Germany, **1998**, chapter 5, p. 203–229.
- [14] S. Ito, T. Kubo, N. Morita, Y. Matsui, T. Watanabe, A. Ohta, K. Fujimori, T. Murafuji, Y. Sugihara, A. Tajiri, *Tetrahedron Lett.* **2004**, *45*, 2891–2894.
- [15] S. Ito, A. Nomura, N. Morita, C. Kabuto, H. Kobayashi, S. Maejima, K. Fujimori, M. Yasunami, *J. Org. Chem.* **2002**, *67*, 7295–7302.
- [16] J.-P. Corbet, G. Mignani, *Chem. Rev.* **2006**, *106*, 2651–2710.
- [17] R. N. McDonald, J. M. Richmond, J. R. Curtis, H. E. Petty, T. L. Hoskins, *J. Org. Chem.* **1976**, *41*, 1811–1821.
- [18] T. Nozoe, S. Seto, S. Matsumura, Y. Murase, *Bull. Chem. Soc. Jpn.* **1962**, *35*, 1179–1188.
- [19] a) P. Suppan, N. Ghoneim, in *Solvochromism*, The Royal Society of Chemistry, Cambridge, **1997**; b) P. Suppan, *J. Photochem. Photobiol. A: Chem.* **1990**, *50*, 293–330; c) R. Christian, in *Solvent and Solvent Effects in Organic Chemistry*, Wiley-VCH, Weinheim, Germany, **2004**.
- [20] a) T. Nozoe, T. Asao, H. Sumumago, M. Ando, *Bull. Chem. Soc. Jpn.* **1974**, *47*, 1471–1476; b) T. Nozoe, T. Asao, M. Yasunami, H. Wakui, T. Suzuki, M. Ando, *J. Org. Chem.* **1996**, *60*, 5919–5924.
- [21] a) S. Hünig, M. Kemmer, H. Wenner, I. F. Perepichka, P. Bäuerle, A. Emge, G. Gescheidt, *Chem. Eur. J.* **1999**, *5*, 1969–1973; b) S. Hünig, M. Kemmer, H.

- Wenner, F. Barbosa, G. Gescheidt, I. F. Perepichka, P. Bäuerle, A. Emge, K. Peters, *Chem. Eur. J.* **2000**, *6*, 2618–2632; c) S. Hünig, I. F. Perepichka, M. Kemmer, H. Wenner, P. Bäuerle, A. Emge, *Tetrahedron* **2000**, *56*, 4203–4211; d) S. Hünig, C. A. Briehn, P. Bäuerle, A. Emge, *Chem. Eur. J.* **2001**, *7*, 2745–2757; e) S. Hünig, A. Langels, M. Schmittel, H. Wenner, I. F. Perepichka, K. Peters, *Eur. J. Org. Chem.* **2001**, 1393–1399.
- [22] a) S. Ito, N. Morita, *Eur. J. Org. Chem.* **2009**, 4567–4579; b) S. Ito, T. Shoji, N. Morita, *Synlett* **2011**, *16*, 2279–2298.
- [23] a) T. Shoji, S. Ito, K. Toyota, T. Iwamoto, M. Yasunami, N. Morita, *Eur. J. Org. Chem.* **2009**, 4316–4324; b) T. Shoji, J. Higashi, S. Ito, T. Okujima, M. Yasunami, N. Morita, *Chem. Eur. J.* **2011**, *17*, 5116–5129; c) T. Shoji, J. Higashi, S. Ito, T. Okujima, M. Yasunami, N. Morita, *Org. Biomol. Chem.* **2012**, *10*, 2431–2438; d) T. Shoji, M. Maruyama, S. Ito, N. Morita, *Bull. Chem. Soc. Jpn.* **2012**, *85*, 761–773.
- [24] The spectroelectrogram measurements were carried out using a two-electrode configuration with a Pt mesh and a wire as the working and counter electrodes, respectively, which were separated by a glass filter. A constant-current reduction and oxidation were applied to the sample solution. The electrical current was monitored by a microampere meter. The potential values are automatically increased by the resistance of the sample solution from 0 V up to ± 12 V, but the potential values could not be monitored by our constant current apparatus.

Received: ((will be filled in by the editorial staff))

Revised: ((will be filled in by the editorial staff))

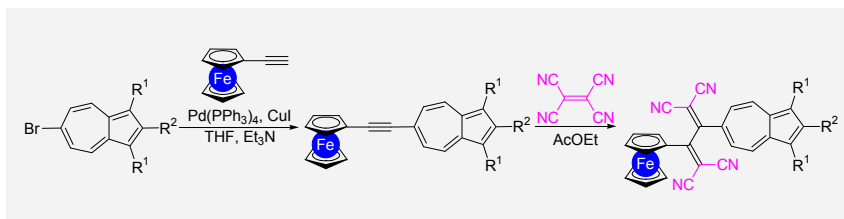
Published online: ((will be filled in by the editorial staff))

Entry for the Table of Contents (Please choose one layout only)

Azulene Chemistry

Taku Shoji,* Shunji Ito, Tetsuo Okujima, Noboru Morita..... Page – Page

Synthesis of 2-Azulenyl-1,1,4,4-tetracyano-3-ferrocenyl-1,3-butadienes by the [2+2] Cycloaddition of (Ferrocenylethynyl)azulenes with Tetracyanoethylene



1-, 2-, and 6-(ferrocenylethynyl)azulenes have been prepared by Sonogashira–Hagihara reaction of ethynylferrocene with the corresponding haloazulenes. These ethynylazulene derivatives reacted with tetracyanoethylene in a [2+2] cycloaddition–cycloreversion reaction to afford the corresponding azulene chromophores in excellent yields.

Significant color change of the novel TCBD derivatives was observed by visible spectroscopy under electrochemical reduction conditions.